

Posterior Mean Super-resolution with a Causal Gaussian Markov Random Field Prior

Takayuki Katsuki, Akira Torii, and Masato Inoue

Abstract—We propose a Bayesian image super-resolution (SR) method with a causal Gaussian Markov random field (MRF) prior. SR is a technique to estimate a spatially high-resolution image from given multiple low-resolution images. An MRF model with the line process supplies a preferable prior for natural images with edges. We improve the existing image transformation model, the compound MRF model, and its hyperparameter prior model. We also logically derive the optimal estimator – not joint maximum a posteriori (MAP) or marginalized maximum likelihood (ML), but posterior mean (PM) – from the objective function of the L2-norm (mean square error) -based peak signal-to-noise ratio (PSNR). Point estimates such as MAP and ML are generally not stable in ill-posed high-dimensional problems because of overfitting, while PM is a stable estimator because all the parameters in the model are evaluated as distributions. The estimator is numerically determined by using variational Bayes. Variational Bayes is a widely used method that approximately determines the complicated posterior distribution without any parameter tuning, but it is generally hard to apply because the conjugate prior is needed. We solve this problem with simple Taylor approximations. Experimental results have shown that the proposed method is more accurate than existing methods.

Index Terms—super-resolution, Bayesian inference, Markov random field prior, line process, posterior mean, variational Bayes, Taylor approximation.

I. INTRODUCTION

Super-resolution (SR) is an information processing technique that makes it possible to infer a spatially high-resolution (HR) image of a scene from corresponding multiple low-resolution (LR) images that are affected by warping, blurring, and noise. SR can be applied for a variety of images; e.g., still images extracted from several sequential video frames. SR needs the registration of LR images in addition to the image restoration of the registered LR images. SR is an ill-posed inverse problem: the degrees of freedom of the system is higher than the dimensionality of the observed LR images, so the complete determination of an HR image is impossible. Therefore, the HR image is frequently inferred as the most preferable image in the framework of the probabilistic information processing. The probabilistic information processing has three key features: 1) model, 2) objective function, and 3) optimization method. In the SR problem, the model includes the observation model and the prior model. The observation model consists of warping, blurring, downsampling, and noise models. The prior model, necessary for the Bayesian

framework, mainly consists of an HR image prior, and sometimes includes both the hyperparameter prior for the HR image prior and the registration prior. The objective function evaluates how good or bad an estimator is. The estimator usually represents the inferred HR image, and sometimes includes auxiliary parameters; e.g., the registration parameters and edge information. The optimization method numerically maximizes/minimizes the objective function and determines the estimator. An optimization method is not necessary for simple problems in which an analytical exact solution can be obtained. Since the earliest work by Tsai and Huang [1], SR has been accomplished using various methods, which can be categorized according to these three key features.

To deal with warping, blurring, and downsampling, a linear transformation model is frequently used. Warping is usually limited with planar rotation and parallel translation. Blurring is defined by using a point spread function (PSF); a square or Gaussian type PSF is common. Downsampling denotes the sampling from an HR image to construct an LR image. Downsampling sometimes includes anti-aliasing. Since these three transformations are linear, they can be combined into a single transformation matrix. As for the noise model, pixel-independent additive white Gaussian noise (AWGN) is usually employed.

The Bayesian framework, especially the HR image prior, is quite useful for SR. The HR image prior provides appropriate smoothness between neighboring pixel luminances. A common type of HR image prior imposes an L2-norm penalty on differences between horizontally and vertically adjacent pixel luminances (the first derivative). The L1-norm of the first derivative is sometimes used, which has the advantage of robust inference against outliers. The TV prior [2] employs the L1-norm of the gradient vector. The Huber prior [3] employs a mixture prior of L1- and L2-norms. The SAR model [4]–[6] employs the response of a two-dimensional Laplacian filter (the second derivative). The Gaussian process prior [7] has neighboring pixels spread according to a Gaussian distribution. In addition to the degree of smoothness between neighboring pixels, information regarding the discontinuity, or equivalently, the edges or line process, is also useful for inference. A common type of prior implementing edges is the compound Markov random field (MRF) prior introduced by Geman & Geman [8], which is widely used in [9]–[11]. With respect to the compound MRF [12], [13] prior, the normalizing constant, or equivalently, the partition function, is usually difficult to calculate because it has an exponential calculation cost with respect to the dimensionality of the line process. Recently, Kanemura et al. [11] confusingly introduced a “causal” type

Takayuki Katsuki, Akira Torii, and Masato Inoue are with the Department of Electrical Engineering and Bioscience, Graduate School of Advanced Science and Engineering, Waseda University, 3-4-1, Okubo, Shinjuku, Tokyo 1698555, Japan e-mail: (see http://www.eb.waseda.ac.jp/m_inoue/).

of Gaussian MRF prior whose calculation cost is polynomial. We try to improve this prior in this paper.

The SR estimator should be derived from an objective function. As the objective function, a posterior distribution has been widely employed. Since the posterior distribution usually includes both the HR image and registration parameters, the joint maximum a posteriori (MAP) solution [4] is a suitable estimator for this objective function. Other than joint MAP, use of marginalized maximum likelihood (ML) [7], [10] or marginalized MAP [3] has been proposed. Tipping et al. and Kanemura et al. determines the registration parameters by ML inference, where the HR image is marginalized out, and determines the HR image by MAP inference. Pickup et al determines the HR image by MAP inference, where the registration uncertainties are marginalized out, and assumes the registration parameters are pre-registered by standard registration techniques. Marginalized ML is also called type II ML, evidence approximation, or empirical Bayes. Marginalized ML has no registration prior, unlike marginalized MAP. Pickup et al. [3] reported that marginalized MAP is superior to both joint MAP and marginalized ML. We evaluate the accuracy of SR methods by L2-norm (mean square error) -based peak signal-to-noise ratio (PSNR). Therefore, we think it is natural to employ PSNR as the objective function. For this objective function, posterior mean (PM) is a suitable estimator. The variational Bayes [14] approach [2] seems to approximately determine the PM of the HR image although they assume some registration parameters are known and use point-estimate model parameters obtained by ML inference. To determine the exact PM of the HR image, all parameters other than the HR image should be marginalized out over the joint posterior distribution.

The type of optimization method to use is not a substantial problem compared to the choice of model and objective function, but it is still important. Since almost all good estimators cannot be exactly determined because of difficult analytical integration or an exponential calculation cost, some approximation methods need to be introduced. Also, parameter tuning is necessary in many numerical optimization methods; e.g., of the initial value and the step-width settings in gradient methods. Specifically, in early work done on image restoration, an annealing method was used for the joint MAP solution [8], [15]. For marginalized ML and marginalized MAP solutions, the scaled conjugate gradients algorithm was used [3], [7]. In recent work, the variational expectation-maximization (EM) algorithm has been applied, which includes a gradient method in M-step [11]. The variational Bayes approach has also been applied [2]. This method includes the nested optimization of the majorization-minimization approach. This majorization-minimization approach seems to affect both the HR image prior and the estimator. Specifically, it modifies the TV prior to include a discontinuity parameter (called local spatial activity). In addition, this parameter is point-estimated when the HR image is inferred.

In this paper, we propose a new SR method that employs a ‘‘causal’’ Gaussian MRF prior and utilizes variational Bayes to calculate the optimal estimator, PM, with respect to the objective function of the L2-norm-based PSNR. This is a

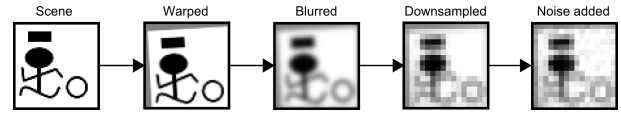


Fig. 1. An illustration of the image observation process

straightforward approach, but possibly it was not proposed earlier because an important limitation of variational Bayes is that a conjugate prior is needed. We solve this problem through simple Taylor approximations. In chapter II, we define models, where we introduce a unified warping, blurring and downsampling model, an improved HR image prior, an improved hyperparameter prior, and a registration prior. In chapter III, we employ PSNR as the objective function, and derive the optimal estimator from this objective function. In chapter IV, we determine the estimator by using variational Bayes and Taylor approximations. In chapter V, we evaluate the proposed method by comparing it to existing methods. In chapter VI, we discuss the advantages of the proposed method. In chapter VII, we conclude.

II. MODEL

A. Definitions

First, we show the definitions of the gamma, Bernoulli, and Gaussian distributions used in this paper:

$$\text{Gamma}(x; a, b) \equiv \frac{b^a}{\Gamma(a)} x^{a-1} e^{-bx} \quad (x > 0),$$

$$\text{Bernoulli}(x; \mu) \equiv \mu^x (1 - \mu)^{1-x} \quad (x \in \{0, 1\}),$$

$$\mathcal{N}(\mathbf{x}; \boldsymbol{\mu}, \boldsymbol{\Sigma}) \equiv |2\pi\boldsymbol{\Sigma}|^{-\frac{1}{2}} e^{-\frac{1}{2}(\mathbf{x}-\boldsymbol{\mu})^T \boldsymbol{\Sigma}^{-1}(\mathbf{x}-\boldsymbol{\mu})} \quad (\mathbf{x} \in \mathcal{R}^d),$$

Here, Γ is the gamma function, $|\bullet|$ denotes the determinant of a given matrix, \mathcal{R} is the real number field, and d is the dimension of \mathbf{x} . Also, the logistic function and Kullback-Leibler (KL) divergence from distribution $p(\mathbf{x})$ to $q(\mathbf{x})$ are respectively defined as

$$\text{logistic}(x) \equiv \frac{1}{1 + e^{-x}},$$

$$D_{\text{KL}}(p(\mathbf{x})||q(\mathbf{x})) \equiv \left\langle \ln \frac{p(\mathbf{x})}{q(\mathbf{x})} \right\rangle_{p(\mathbf{x})},$$

where the angle brackets $\langle \bullet \rangle_{\circ}$ denote the expectation of \bullet with respect to a distribution \circ . Also, tr denotes the trace of a given matrix. Superscript T denotes the transpose. diag denotes a diagonal matrix. \mathbf{I} is an identity matrix of appropriate size. $\mathbf{0}$ is a zero vector or a zero matrix of appropriate size. All the vectors in this paper are column vectors. $\|\bullet\|_2$ denotes the L2-norm of a given vector. At this point, these variables have absolutely nothing to do with the variables that appear later.

B. Observation Model

Our task is to estimate an HR grayscale image $\mathbf{x} \in \mathcal{R}^{N_x}$ from observed multiple LR grayscale images $\mathbf{Y} \equiv \{\mathbf{y}_l\}_{l=1}^L$, $\mathbf{y}_l \in \mathcal{R}^{N_y}$. The images \mathbf{y}_l and \mathbf{x} are regarded as lexicographically stacked vectors. The number of pixels for each LR image is assumed to be less than that of the HR image; i.e.,

$N_y < N_x$. We do this estimation using an SR technique whose resolution enhancement factor is $\alpha \equiv \sqrt{N_x/N_y}$. Although we define the range of a pixel luminance value as infinite, we use -1 for black, $+1$ for white, and values between -1 and $+1$ for gradual gray.

The image observation process is modeled as shown in Fig. 1; the HR image \mathbf{x} is geometrically warped, blurred, downsampled, and corrupted by noise ϵ_l to form the observed LR image \mathbf{y}_l :

$$\mathbf{y}_l \equiv \mathbf{W}(\phi_l)\mathbf{x} + \epsilon_l, \quad (1)$$

or, more strictly,

$$p(\mathbf{Y}|\mathbf{x}, \beta, \Phi) \equiv \prod_{l=1}^L \mathcal{N}(\mathbf{y}_l; \mathbf{W}(\phi_l)\mathbf{x}, \beta^{-1}\mathbf{I}). \quad (2)$$

The $\epsilon_l \in \mathcal{R}^{N_y}$ is AWGN with precision (inverse variance) β (> 0). Here, $\mathbf{W}(\phi_l)$ is the transformation matrix that operates warping, blurring, and downsampling simultaneously. It is defined as

$$\mathbf{W}(\phi_l)_{i,j} \equiv \frac{\exp\left(-\frac{\gamma}{2}\|\vec{k}\|_2^2\right)}{\vartheta_3\left(\vec{k}_x, e^{-\frac{2\pi^2}{\gamma}}\right)\vartheta_3\left(\vec{k}_y, e^{-\frac{2\pi^2}{\gamma}}\right)}, \quad (3)$$

$$\vec{k} \equiv \begin{bmatrix} \cos\theta_l & \sin\theta_l \\ -\sin\theta_l & \cos\theta_l \end{bmatrix} \left(\alpha\vec{i} - \vec{o}_l\right) - \vec{j}, \quad (4)$$

$$\vartheta_3(u, q) \equiv 1 + 2 \sum_{n=1}^{\infty} q^{n^2} \cos 2n\pi u, \quad (5)$$

where vectors \vec{i} and \vec{j} denote the two-dimensional positions of the i -th pixel of the observed LR image and the j -th pixel of the original HR image, respectively. Subscripts x and y respectively denote horizontal and vertical positions on the image. Here, we define the center of each image as the origin. We also define that the size of each pixel is 1 by 1. ϑ_3 is the elliptic theta function. We introduce it as the normalizing constant for sampling from a Gaussian distribution at regular intervals. This normalizing constant is derived under the assumption that the HR image has an infinite number of 0 (middle gray) pixels around N_x pixels. Especially on the marginal portion of the HR image, the elliptic theta function enables more favorable normalization than what has been achieved elsewhere [7], [11]. ϕ_l is a four-dimensional vector consisting of the transformation parameters: rotational motion parameter θ_l , translational motion parameter \vec{o}_l , and blurring parameter γ_l .

$$\Phi \equiv \{\phi_l\}_{l=1}^L, \quad \phi_l \equiv [\phi_{l,k}]_{k=1}^4 \equiv [\theta_l, [\vec{o}_l]_x, [\vec{o}_l]_y, \gamma_l]^T. \quad (6)$$

In this paper, we assume γ_l differs for each observed image.

C. HR Image Prior

Here, we introduce a ‘‘causal’’ Gaussian MRF prior for the HR image and additional latent variables. These latent variables are called the line process that controls the local correlation among pixel luminances. The introduction of the latent variables enables explicit expression of the possible discontinuity in the HR image. The

line process $\boldsymbol{\eta}$ consists of binary latent variables $\eta_{i,j} \in \{0, 1\}$ for all adjacent pixel pairs i and j . Its size equals $N_\eta \equiv 2 \times [\text{number of HR image's horizontal pixels} - 1] \times [\text{number of HR image's vertical pixels} - 1]$. We define the prior as

$$p(\mathbf{x}, \boldsymbol{\eta}|\lambda, \rho, \kappa) \equiv p(\mathbf{x}|\boldsymbol{\eta}, \rho, \kappa)p(\boldsymbol{\eta}|\lambda) \quad (7)$$

$$= \exp \left[-\lambda \sum_{i \sim j} (1 - \eta_{i,j}) - \frac{\rho}{2} \sum_{i \sim j} \eta_{i,j} (x_i - x_j)^2 - \frac{\kappa}{2} \|\mathbf{x}\|_2^2 + \frac{1}{2} \ln \left| \frac{\mathbf{A}(\boldsymbol{\eta}, \rho, \kappa)}{2\pi} \right| + N_\eta \ln \text{logistic}(\lambda) \right], \quad (8)$$

where

$$p(\boldsymbol{\eta}|\lambda) \equiv \prod_{i \sim j} \text{Bernoulli}(\eta_{i,j}; \text{logistic}(\lambda)), \quad (9)$$

$$p(\mathbf{x}|\boldsymbol{\eta}, \rho, \kappa) \equiv \mathcal{N}(\mathbf{x}; \mathbf{0}, \mathbf{A}(\boldsymbol{\eta}, \rho, \kappa)^{-1}), \quad (10)$$

$$\mathbf{A}(\boldsymbol{\eta}, \rho, \kappa)_{i,j} \equiv \begin{cases} \rho \sum_{k \sim i} \eta_{i,k} + \kappa, & i = j, \\ -\rho \eta_{i,j}, & i \sim j, \\ 0, & \text{otherwise.} \end{cases} \quad (11)$$

Here, the summation $\sum_{i \sim j}$ is taken over all pairs of adjacent pixels. The notation $i \sim j$ means that the i -th and the j -th pixels are adjacent in upward, downward, leftward, and rightward directions. The line process $\boldsymbol{\eta}$ switches the local characteristics of the prior. It indicates whether two adjacent pixels take similar values or independent values. When $\eta_{i,j} = 1$, the i -th and the j -th pixels are strongly smoothed according to the quadratic penalty, whereas there is no smoothing when $\eta_{i,j} = 0$. The hyperparameter λ (> 0) is an edge penalty parameter which prevents $\eta_{i,j}$ from excessively taking edges. Note that λ is restricted to positive because negative λ leads to a reward rather than a penalty for taking edges. Also, ρ (> 0) is a smoothness parameter which prevents the differences of adjacent pixel luminances from becoming large, and κ (> 0) is a contrast parameter which prevents \mathbf{x} from taking an improperly large absolute value. $\mathbf{A}(\boldsymbol{\eta}, \rho, \kappa)$ is the $N_x \times N_x$ precision matrix of \mathbf{x} .

We have defined the joint distribution of \mathbf{x} and $\boldsymbol{\eta}$ in the form of $p(\boldsymbol{\eta})p(\mathbf{x}|\boldsymbol{\eta})$. We call such a model ‘‘causal’’ because $\boldsymbol{\eta}$ seems to cause \mathbf{x} . The MRF model is defined as having the property

$$p(x_i|\mathbf{x} \setminus x_i, \boldsymbol{\eta}) = p(x_i|\mathbf{x}_{\mathcal{L}(i)}, \boldsymbol{\eta}_{i, \mathcal{L}(i)}) \quad (12)$$

in this case; i.e., the conditional distribution of a random variable, x_i , given all other variables, $\mathbf{x} \setminus x_i$ and $\boldsymbol{\eta}$, equals the conditional distribution of the random variable given its ‘‘neighboring’’ variables, $\mathbf{x}_{\mathcal{L}(i)}$ and $\boldsymbol{\eta}_{i, \mathcal{L}(i)}$. If this conditional distribution is a Gaussian distribution, such an MRF is called a Gaussian MRF.

The ‘‘compound’’ MRF prior is usually defined in the form of the Gibbs distribution [8],

$$\tilde{p}(\mathbf{x}, \boldsymbol{\eta}) \equiv \frac{\exp(-\tilde{H}(\mathbf{x}, \boldsymbol{\eta}))}{\sum_{\boldsymbol{\eta}} \int \exp(-\tilde{H}(\mathbf{x}, \boldsymbol{\eta})) d\mathbf{x}}, \quad (13)$$

which is based on some microstate energy function, or equivalently, a Hamiltonian, such as

$$\begin{aligned} \tilde{H}(\mathbf{x}, \boldsymbol{\eta}) \\ \equiv \lambda \sum_{i \sim j} (1 - \eta_{i,j}) + \frac{\rho}{2} \sum_{i \sim j} \eta_{i,j} (x_i - x_j)^2 + \frac{\kappa}{2} \|\mathbf{x}\|_2^2. \end{aligned} \quad (14)$$

In addition to the property of Eq. (12), a compound MRF also has the property of

$$\tilde{p}(\eta_{i,j} | \mathbf{x}, \boldsymbol{\eta} \setminus \eta_{i,j}) = \tilde{p}(\eta_{i,j} | x_i, x_j), \quad (15)$$

whereas the proposed causal Gaussian MRF prior does not. Therefore, we do not call the proposed prior a ‘‘compound’’ MRF prior.

D. Hyperparameter Prior

Generally, prior distributions should be non-informative unless we have explicit reasons because an informative prior leads to heuristics. Actually, we define the prior distributions for the hyperparameters of the HR image prior to be as non-informative as possible,

$$\begin{aligned} p(\lambda, \rho, \kappa, \beta) \equiv & \text{Gamma}(\lambda; a_\lambda^{(0)}, b_\lambda^{(0)}) \text{Gamma}(\rho; a_\rho^{(0)}, b_\rho^{(0)}) \\ & \times \text{Gamma}(\kappa; a_\kappa^{(0)}, b_\kappa^{(0)}) \text{Gamma}(\beta; a_\beta^{(0)}, b_\beta^{(0)}), \end{aligned} \quad (16)$$

$$\begin{aligned} a_\lambda^{(0)} \equiv 10^{-2}, b_\lambda^{(0)} \equiv 10^{-2}, a_\rho^{(0)} \equiv 10^{-2}, b_\rho^{(0)} \equiv 10^{-2}, \\ a_\kappa^{(0)} \equiv 10^{-2}, b_\kappa^{(0)} \equiv 10^{-2}, a_\beta^{(0)} \equiv 10^{-2}, b_\beta^{(0)} \equiv 10^{-2}. \end{aligned} \quad (17)$$

For a gamma distribution, the number of effective prior observations in the Bayesian framework is equal to two times parameter a . As shown later, the number of observations for the hyperparameter λ is N_η in this SR. Also, that for ρ and κ is N_x , and that for β is LN_y . Therefore, the above settings – e.g., $2a_\lambda^{(0)} \ll N_\eta$ – are considered sufficiently non-informative.

E. Registration Prior

For the registration parameters including the blurring parameter, we also define the corresponding prior as

$$p(\Phi) \equiv \prod_{l=1}^L \mathcal{N}(\phi_l; \boldsymbol{\mu}_{\phi_l}^{(0)}, \boldsymbol{\Sigma}_{\phi_l}^{(0)}), \quad (18)$$

$$\boldsymbol{\mu}_{\phi_l}^{(0)} \equiv [0, 0, 0, 12/\alpha^2], \boldsymbol{\Sigma}_{\phi_l}^{(0)} \equiv \text{diag}[10^{-3}, 10^0, 10^0, 10^{-3}]. \quad (19)$$

For the rotation parameter θ_l , the prior assumes 0 ± 1.81 degree ($\frac{180}{\pi} \sqrt{10^{-3}} \simeq 1.81$). This is considered suitable for this SR task. Similarly, an assumption of 0 ± 1 pixels for $[\bar{\sigma}_l]_x$ and $[\bar{\sigma}_l]_y$ is considered suitable. For the blurring parameter γ_l , $\mu_{\gamma_l}^{(0)}$ is derived as the value equivalent to the anti-aliasing of the scale factor α .

For simplicity, we also define the mean value for the gamma distribution as

$$\mu_\lambda^{(\dagger)} \equiv \frac{a_\lambda^{(\dagger)}}{b_\lambda^{(\dagger)}}, \mu_\rho^{(\dagger)} \equiv \frac{a_\rho^{(\dagger)}}{b_\rho^{(\dagger)}}, \mu_\kappa^{(\dagger)} \equiv \frac{a_\kappa^{(\dagger)}}{b_\kappa^{(\dagger)}}, \mu_\beta^{(\dagger)} \equiv \frac{a_\beta^{(\dagger)}}{b_\beta^{(\dagger)}}.$$

III. OBJECTIVE FUNCTION AND ESTIMATOR

A. Peak Signal-to-Noise Ratio (PSNR)

First, we confirm that the joint distribution of all random variables can now be explicitly given as

$$p(\mathbf{Y}, \mathbf{z}) = p(\mathbf{Y} | \mathbf{x}, \beta, \Phi) p(\mathbf{x}, \boldsymbol{\eta} | \lambda, \rho, \kappa) p(\lambda, \rho, \kappa, \beta) p(\Phi), \quad (20)$$

$$\mathbf{z} \equiv [\mathbf{x}, \boldsymbol{\eta}, [\lambda, \rho, \kappa, \beta], \Phi], \quad (21)$$

Once the joint distribution is obtained, we can derive all the marginal and conditional distributions; e.g., the posterior distribution $p(\mathbf{z} | \mathbf{Y})$ and joint distribution of the HR and LR images $p(\mathbf{Y}, \mathbf{x})$.

One of the most commonly used evaluation functions of the inferred image would be the L2-norm (mean square error)-based PSNR. It is defined as

$$\text{PSNR}(\hat{\mathbf{x}}; \mathbf{x}) \equiv 10 \log_{10} \frac{2^2}{\frac{1}{N_x} \|\hat{\mathbf{x}} - \mathbf{x}\|_2^2}, \quad (22)$$

where $\hat{\mathbf{x}}$ is the estimator of the HR image and \mathbf{x} is the true HR image. Since only LR images, \mathbf{Y} , are available for the estimator, we sometimes explicitly express it as a function form, $\hat{\mathbf{x}}(\mathbf{Y})$. Now, our objective function (functional) to maximize regarding the estimator is defined as

$$\langle \text{PSNR}(\hat{\mathbf{x}}(\mathbf{Y}); \mathbf{x}) \rangle_{p(\mathbf{Y}, \mathbf{x})}. \quad (23)$$

This is because we prefer good estimator performance on average over various HR images and the corresponding LR images. Here, we assume that the occurrence rate of HR and LR images exactly coincides with the model we just introduced.

B. Posterior Mean (PM)

Using the objective function above, we can explicitly derive the best estimator of the HR image as the PM,

$$\underset{\hat{\mathbf{x}}(\mathbf{Y})}{\text{argmax}} \langle \text{PSNR}(\hat{\mathbf{x}}(\mathbf{Y}); \mathbf{x}) \rangle_{p(\mathbf{Y}, \mathbf{x})} = \langle \mathbf{x} \rangle_{p(\mathbf{x} | \mathbf{Y})}. \quad (24)$$

Note that $p(\mathbf{x} | \mathbf{Y})$ needs marginalization of all parameters other than \mathbf{x} over $p(\mathbf{z} | \mathbf{Y})$. If the PM of the line process or other model parameters is necessary, it can also be determined in the same manner.

IV. OPTIMIZATION METHOD

A. Variational Bayes

Though we could derive the optimal estimator, we cannot obtain the analytical solutions of the posterior distribution $p(\mathbf{z} | \mathbf{Y})$ and marginalized posterior distribution $p(\mathbf{x} | \mathbf{Y})$. Consequently, we have to rely on approximation. Here, we employ the variational Bayes.

The variational Bayes [14] provides a trial distribution $q(\mathbf{z})$ that approximates the true posterior. We impose the factorization assumption on the trial distribution,

$$q(\mathbf{z}) \equiv q(\mathbf{x}) q(\boldsymbol{\eta}) q(\lambda, \rho, \kappa, \beta) q(\Phi). \quad (25)$$

Note that, at this moment, the distribution family of each factorized distribution is not limited. We identify the optimal

trial distribution that minimizes the KL divergence between the trial and the true distributions as the best approximation of the true distribution:

$$\hat{q}(\mathbf{z}) \equiv \operatorname{argmin}_{q(\mathbf{z})} D_{\text{KL}}(q(\mathbf{z}) \| p(\mathbf{z} | \mathbf{Y})). \quad (26)$$

Actually, the trial distribution that minimizes the inverse KL distance coincides with the product of the exact marginal distributions,

$$\operatorname{argmin}_{q(\mathbf{z})} D_{\text{KL}}(p(\mathbf{z} | \mathbf{Y}) \| q(\mathbf{z})) = \prod_i p(z_i | \mathbf{Y}), \quad (27)$$

but this minimization is difficult to calculate.

Under the factorization assumption of trial distribution and the extremal condition of KL divergence, each optimal trial distribution should satisfy the self-consistent equations,

$$\hat{q}(z_i) \propto \exp(\ln p(\mathbf{z} | \mathbf{Y})) \prod_{j \neq i} \hat{q}(z_j). \quad (28)$$

In the common style of variational Bayes, this equation is solved by repetitive updates,

$$q^{(0)}(z_i) \equiv p(z_i), \quad (29)$$

$$q^{(t+1)}(z_i) \propto \exp(\ln p(\mathbf{z} | \mathbf{Y})) \prod_{j \neq i} q^{(t)}(z_j). \quad (30)$$

Each factorized trial distribution is supposed to converge to the optimal distribution. Sometimes, some $q^{(t+1)}(z_i)$ are used instead of $q^{(t)}(z_i)$ for the distribution on the right-hand side of Eq. (30). It depends on the hierarchical structure of the model. Similarly, some $q^{(0)}(z_i)$ may not be necessary.

B. Taylor Approximations

Although the variational Bayes is a widely used general framework, its application is difficult in practice because it demands a conjugate prior. The prior distributions we have introduced are not conjugate priors. However, we have found that simple Taylor approximations make them conjugate. These approximations also enable the analytical exact expectations in Eq. (30).

Specifically, we apply the first order Taylor approximation for three non-linear terms. $\mathbf{W}(\phi_l)$ is approximated around $\phi_l = \boldsymbol{\mu}_{\phi_l}^{(t)}$,

$$\mathbf{W}(\phi_l) \simeq \mathbf{W}_l^{(t)} + \sum_{k=1}^4 [\phi_l - \boldsymbol{\mu}_{\phi_l}^{(t)}]_k \mathbf{W}'_{l,k}{}^{(t)}, \quad (31)$$

where

$$\mathbf{W}_l^{(t)} \equiv \mathbf{W}(\boldsymbol{\mu}_{\phi_l}^{(t)}), \quad (32)$$

$$\mathbf{W}'_{l,k}{}^{(t)} \equiv \left. \frac{\partial \mathbf{W}(\phi_l)}{\partial \phi_{l,k}} \right|_{\phi_l = \boldsymbol{\mu}_{\phi_l}^{(t)}}. \quad (33)$$

Similarly, $\ln |\mathbf{A}(\boldsymbol{\eta}, \rho, \kappa)|$ is approximated around $[\boldsymbol{\eta}, \ln \rho, \ln \kappa] = [\boldsymbol{\mu}_{\boldsymbol{\eta}}^{(t)}, \ln \mu_{\rho}^{(t)}, \ln \mu_{\kappa}^{(t)}]$,

$$\begin{aligned} \ln |\mathbf{A}(\boldsymbol{\eta}, \rho, \kappa)| &\simeq \ln |\mathbf{A}(\boldsymbol{\mu}_{\boldsymbol{\eta}}^{(t)}, \mu_{\rho}^{(t)}, \mu_{\kappa}^{(t)})| \\ &+ \operatorname{tr} \mathbf{A}(\boldsymbol{\mu}_{\boldsymbol{\eta}}^{(t)}, \mu_{\rho}^{(t)}, \mu_{\kappa}^{(t)})^{-1} \left[\mu_{\rho}^{(t)} \mathbf{A}'(\boldsymbol{\eta} - \boldsymbol{\mu}_{\boldsymbol{\eta}}^{(t)}) \right. \\ &\left. + (\ln \rho - \ln \mu_{\rho}^{(t)}) \mu_{\rho}^{(t)} \mathbf{A}'(\mu_{\rho}^{(t)}) + (\ln \kappa - \ln \mu_{\kappa}^{(t)}) \mu_{\kappa}^{(t)} \mathbf{I} \right], \quad (34) \end{aligned}$$

where

$$\mathbf{A}'(\boldsymbol{\eta}) \equiv \mathbf{A}(\boldsymbol{\eta}, 1, 0) = \sum_{i \sim j} \eta_{i,j} \mathbf{M}_{i,j}, \quad (35)$$

$$[\mathbf{M}_{i,j}]_{k,l} \equiv \begin{cases} +1, & (k,l) = (i,i) \text{ or } (j,j), \\ -1, & (k,l) = (i,j) \text{ or } (j,i), \\ 0, & \text{otherwise.} \end{cases} \quad (36)$$

We also use a similar approximation around $[\boldsymbol{\eta}, \ln \rho, \ln \kappa] = [\boldsymbol{\mu}_{\boldsymbol{\eta}}^{(t+1)}, \ln \mu_{\rho}^{(t)}, \ln \mu_{\kappa}^{(t)}]$. In addition, $\ln \operatorname{logistic}(\lambda)$ is approximated around $\ln \lambda = \ln \mu_{\lambda}^{(t)}$,

$$\begin{aligned} \ln \operatorname{logistic}(\lambda) &\simeq \ln \operatorname{logistic}(\mu_{\lambda}^{(t)}) \\ &+ (\ln \lambda - \ln \mu_{\lambda}^{(t)}) \mu_{\lambda}^{(t)} \operatorname{logistic}(-\mu_{\lambda}^{(t)}). \quad (37) \end{aligned}$$

C. Update Equations

From Eqs. (29-37), the trial distributions are obtained as the following distributions:

$$q^{(t)}(\boldsymbol{\eta}) = \prod_{i \sim j} \operatorname{Bernoulli}(\eta_{i,j}; \mu_{\eta_{i,j}}^{(t)}) \quad (38)$$

$$q^{(t)}(\mathbf{x}) = \mathcal{N}(\mathbf{x}; \boldsymbol{\mu}_{\mathbf{x}}^{(t)}, \boldsymbol{\Sigma}_{\mathbf{x}}^{(t)}) \quad (39)$$

$$\begin{aligned} q^{(t)}(\lambda, \rho, \kappa, \beta) &= \operatorname{Gamma}(\lambda; a_{\lambda}^{(t)}, b_{\lambda}^{(t)}) \operatorname{Gamma}(\rho; a_{\rho}^{(t)}, b_{\rho}^{(t)}) \\ &\times \operatorname{Gamma}(\kappa; a_{\kappa}^{(t)}, b_{\kappa}^{(t)}) \operatorname{Gamma}(\beta; a_{\beta}^{(t)}, b_{\beta}^{(t)}) \quad (40) \end{aligned}$$

$$q^{(t)}(\boldsymbol{\Phi}) = \prod_{l=1}^L \mathcal{N}(\phi_l; \boldsymbol{\mu}_{\phi_l}^{(t)}, \boldsymbol{\Sigma}_{\phi_l}^{(t)}). \quad (41)$$

For Eq. (30), we do the following. First, we compute $q^{(t+1)}(\boldsymbol{\eta})$ using $q^{(t)}(\mathbf{x}, \lambda, \rho, \kappa, \beta, \boldsymbol{\Phi})$. Second, we compute $q^{(t+1)}(\mathbf{x})$ using $q^{(t+1)}(\boldsymbol{\eta}) q^{(t)}(\lambda, \rho, \kappa, \beta, \boldsymbol{\Phi})$. In the end, we compute $q^{(t+1)}(\lambda, \rho, \kappa, \beta)$ using $q^{(t+1)}(\mathbf{x}, \boldsymbol{\eta}) q^{(t)}(\boldsymbol{\Phi})$ and $q^{(t+1)}(\boldsymbol{\Phi})$ using $q^{(t+1)}(\mathbf{x}, \boldsymbol{\eta}) q^{(t)}(\lambda, \rho, \kappa, \beta)$. For the initial parameters of the trial distributions of $\boldsymbol{\eta}$ and \mathbf{x} , we use non-informative values,

$$\boldsymbol{\mu}_{\boldsymbol{\eta}}^{(0)} \equiv \mathbf{0}, \quad \boldsymbol{\mu}_{\mathbf{x}}^{(0)} \equiv \mathbf{0}, \quad \boldsymbol{\Sigma}_{\mathbf{x}}^{(0)} \equiv \mathbf{0}. \quad (42)$$

As the initial parameters for $\lambda, \rho, \beta, \kappa$ and $\boldsymbol{\Phi}$, we used the same values as their prior's values.

Here, we show each distribution in detail. The update equation of $\boldsymbol{\eta}$ is given as

$$\begin{aligned} q^{(t+1)}(\boldsymbol{\eta}) &\propto \exp(\ln p(\mathbf{z} | \mathbf{Y}))_{q^{(t)}(\mathbf{x}, \lambda, \rho, \kappa, \beta, \boldsymbol{\Phi})} \\ &\propto \exp \left(\sum_{i \sim j} \left\{ c_{\lambda}^{(t)} - \frac{\mu_{\rho}^{(t)}}{2} \operatorname{tr} \mathbf{C}_{\mathbf{x}}^{(t)} \mathbf{M}_{i,j} \right\} \eta_{i,j} \right. \\ &\left. + \frac{1}{2} (\ln |\mathbf{A}(\boldsymbol{\eta}, \rho, \kappa)|)_{q^{(t)}(\rho, \kappa)} \right), \quad (43) \end{aligned}$$

where

$$\mathbf{C}_{\mathbf{x}}^{(t)} \equiv \boldsymbol{\mu}_{\mathbf{x}}^{(t)} [\boldsymbol{\mu}_{\mathbf{x}}^{(t)}]^T + \boldsymbol{\Sigma}_{\mathbf{x}}^{(t)}. \quad (44)$$

Using the Taylor approximation (34), we obtain the distribution of Eq. (38) at step $t+1$ with the parameter of

$$\mu_{\eta_{i,j}}^{(t+1)} = \operatorname{logistic} \left(\mu_{\lambda}^{(t)} + \frac{1}{2} \mu_{\rho}^{(t)} c_{\eta_{i,j}}^{(t)} \right), \quad (45)$$

where

$$\mathbf{C}_{\eta_{i,j}}^{(\theta)} \equiv \text{tr} \left[\left(\mathbf{A}(\boldsymbol{\mu}_\eta^{(\theta)}, \mu_\rho^{(\theta)}, \mu_\kappa^{(\theta)})^{-1} - \mathbf{C}_x^{(\theta)} \right) \mathbf{M}_{i,j} \right]. \quad (46)$$

The update equation of \mathbf{x} is given as

$$\begin{aligned} q^{(\theta+1)}(\mathbf{x}) &\propto \exp \langle \ln p(\mathbf{z}|\mathbf{Y}) \rangle_{q^{(\theta+1)}(\boldsymbol{\eta})q^{(\theta)}(\lambda, \rho, \kappa, \beta, \Phi)} \\ &\propto \exp \left(-\frac{1}{2} \left\{ \mathbf{x}^T \mathbf{A}(\boldsymbol{\mu}_\eta^{(\theta+1)}, \mu_\rho^{(\theta)}, \mu_\kappa^{(\theta)}) \mathbf{x} \right. \right. \\ &\quad \left. \left. + \mu_\beta^{(\theta)} \sum_{l=1}^L \langle \|\mathbf{W}(\phi_l)\mathbf{x} - \mathbf{y}_l\|_2^2 \rangle_{q^{(\theta)}(\phi_l)} \right\} \right). \end{aligned} \quad (47)$$

It becomes a Gaussian distribution. Using the Taylor approximation (31), we obtain the distribution of Eq. (39) at step $t+1$ with the parameters of

$$\boldsymbol{\mu}_x^{(\theta+1)} = \boldsymbol{\Sigma}_x^{(\theta+1)} \left[\mu_\beta^{(\theta)} \sum_{l=1}^L \mathbf{y}_l^T \mathbf{W}_l^{(\theta)} \right]^T, \quad (48)$$

$$\boldsymbol{\Sigma}_x^{(\theta+1)} = \left[\mathbf{A}(\boldsymbol{\mu}_\eta^{(\theta+1)}, \mu_\rho^{(\theta)}, \mu_\kappa^{(\theta)}) + \mu_\beta^{(\theta)} \sum_{l=1}^L \mathbf{C}_{\mathbf{W}_l}^{(\theta)} \right]^{-1}, \quad (49)$$

where

$$\mathbf{C}_{\mathbf{W}_l}^{(\theta)} \equiv [\mathbf{W}_l^{(\theta)}]^T \mathbf{W}_l^{(\theta)} + \sum_{k,k'} [\boldsymbol{\Sigma}_{\phi_l}^{(\theta)}]_{k,k'} [\mathbf{W}'_{l,k}{}^{(\theta)}]^T \mathbf{W}'_{l,k'}{}^{(\theta)}. \quad (50)$$

The update equation of $\lambda, \rho, \kappa, \beta$ is given as

$$\begin{aligned} q^{(\theta+1)}(\lambda, \rho, \kappa, \beta) &\propto \exp \langle \ln p(\mathbf{z}|\mathbf{Y}) \rangle_{q^{(\theta+1)}(\mathbf{x}, \boldsymbol{\eta})q^{(\theta)}(\Phi)} \\ &\propto \lambda^{a_\lambda^{(0)} - 1} \rho^{a_\rho^{(0)} - 1} \kappa^{a_\kappa^{(0)} - 1} \beta^{a_\beta^{(0)} + \frac{1}{2}LN\mathbf{y}} \exp \left(\right. \\ &\quad - \left\{ b_\lambda^{(0)} + \sum_{i \sim j} (1 - \mu_{\eta_{i,j}}^{(\theta+1)}) \right\} \lambda \\ &\quad - \left\{ b_\rho^{(0)} + \frac{1}{2} \text{tr} \mathbf{C}_x^{(\theta+1)} \mathbf{A}'(\boldsymbol{\mu}_\eta^{(\theta+1)}) \right\} \rho \\ &\quad - \left\{ b_\kappa^{(0)} + \frac{1}{2} \text{tr} \mathbf{C}_x^{(\theta+1)} \right\} \kappa \\ &\quad - \left\{ b_\beta^{(0)} + \frac{1}{2} \sum_{l=1}^L \left\langle \text{tr} \mathbf{C}_x^{(\theta+1)} \mathbf{W}(\phi_l)^T \mathbf{W}(\phi_l) \right. \right. \\ &\quad \left. \left. - 2\mathbf{y}_l^T \mathbf{W}(\phi_l) \boldsymbol{\mu}_x^{(\theta+1)} + \mathbf{y}_l^T \mathbf{y}_l \right\rangle_{q^{(\theta)}(\phi_l)} \right\} \beta \\ &\quad \left. + \frac{1}{2} \langle \ln |\mathbf{A}(\boldsymbol{\eta}, \rho, \kappa)| \rangle_{q^{(\theta+1)}(\boldsymbol{\eta})} + N_\eta \ln \text{logistic}(\lambda) \right). \end{aligned} \quad (51)$$

Using Taylor approximations (31), (34), and (37), we obtain

the distribution of Eq. (40) at step $t+1$ with parameters of

$$a_\lambda^{(\theta+1)} = a_\lambda^{(0)} + N_\eta \mu_\lambda^{(\theta)} \text{logistic}(-\mu_\lambda^{(\theta)}), \quad (52)$$

$$b_\lambda^{(\theta+1)} = b_\lambda^{(0)} + \sum_{i \sim j} (1 - \mu_{\eta_{i,j}}^{(\theta+1)}), \quad (53)$$

$$a_\rho^{(\theta+1)} = a_\rho^{(0)} + \frac{\mu_\rho^{(\theta)}}{2} \text{tr} \mathbf{A}(\boldsymbol{\mu}_\eta^{(\theta+1)}, \mu_\rho^{(\theta)}, \mu_\kappa^{(\theta)})^{-1} \mathbf{A}'(\boldsymbol{\mu}_\eta^{(\theta+1)}) \quad (54)$$

$$b_\rho^{(\theta+1)} = b_\rho^{(0)} + \frac{1}{2} \text{tr} \mathbf{C}_x^{(\theta+1)} \mathbf{A}'(\boldsymbol{\mu}_\eta^{(\theta+1)}), \quad (55)$$

$$a_\kappa^{(\theta+1)} = a_\kappa^{(0)} + \frac{\mu_\kappa^{(\theta)}}{2} \text{tr} \mathbf{A}(\boldsymbol{\mu}_\eta^{(\theta+1)}, \mu_\rho^{(\theta)}, \mu_\kappa^{(\theta)})^{-1} \quad (56)$$

$$b_\kappa^{(\theta+1)} = b_\kappa^{(0)} + \frac{1}{2} \text{tr} \mathbf{C}_x^{(\theta+1)}, \quad (57)$$

$$a_\beta^{(\theta+1)} = a_\beta^{(0)} + \frac{1}{2} LN\mathbf{y}, \quad (58)$$

$$b_\beta^{(\theta+1)} = b_\beta^{(0)} + \frac{1}{2} \sum_{l=1}^L \left(\text{tr} \mathbf{C}_x^{(\theta+1)} \mathbf{C}_{\mathbf{W}_l}^{(\theta)} - 2\mathbf{y}_l^T \mathbf{W}_l^{(\theta)} \boldsymbol{\mu}_x^{(\theta+1)} + \mathbf{y}_l^T \mathbf{y}_l \right). \quad (59)$$

The update equation of Φ is given as

$$q^{(\theta+1)}(\Phi) \propto \exp \langle \ln p(\mathbf{z}|\mathbf{Y}) \rangle_{q^{(\theta+1)}(\mathbf{x}, \boldsymbol{\eta})q^{(\theta)}(\lambda, \rho, \kappa, \beta)} \quad (60)$$

$$\begin{aligned} &\propto \exp \left(-\frac{1}{2} \sum_{l=1}^L \left\{ [\phi_l - \boldsymbol{\mu}_{\phi_l}^{(0)}]^T [\boldsymbol{\Sigma}_{\phi_l}^{(0)}]^{-1} [\phi_l - \boldsymbol{\mu}_{\phi_l}^{(0)}] \right. \right. \\ &\quad \left. \left. + \mu_\beta^{(\theta)} \left\{ \text{tr} \mathbf{C}_x^{(\theta+1)} \mathbf{W}(\phi_l)^T \mathbf{W}(\phi_l) - 2\mathbf{y}_l^T \mathbf{W}(\phi_l) \boldsymbol{\mu}_x^{(\theta+1)} \right\} \right\} \right). \end{aligned}$$

Using the Taylor approximation (31), we obtain the distribution of Eq. (41) at step $t+1$ with parameters of

$$\boldsymbol{\mu}_{\phi_l}^{(\theta+1)} = \boldsymbol{\Sigma}_{\phi_l}^{(\theta+1)} \left[[\boldsymbol{\Sigma}_{\phi_l}^{(0)}]^{-1} \boldsymbol{\mu}_{\phi_l}^{(0)} + \mu_\beta^{(\theta)} [\mathbf{C}_{\phi_l}''^{(\theta+1)} \boldsymbol{\mu}_{\phi_l}^{(\theta)} - \mathbf{C}_{\phi_l}^{(\theta+1)}] \right], \quad (61)$$

$$\boldsymbol{\Sigma}_{\phi_l}^{(\theta+1)} = \left[[\boldsymbol{\Sigma}_{\phi_l}^{(0)}]^{-1} + \mu_\beta^{(\theta)} \mathbf{C}_{\phi_l}''^{(\theta+1)} \right]^{-1}, \quad (62)$$

where

$$\begin{aligned} [\mathbf{C}_{\phi_l}'^{(\theta+1)}]_k &\equiv \frac{1}{2} \text{tr} \mathbf{C}_x^{(\theta+1)} \left[[\mathbf{W}_l^{(\theta)}]^T \mathbf{W}'_{l,k}{}^{(\theta)} + [\mathbf{W}'_{l,k}{}^{(\theta)}]^T \mathbf{W}_l^{(\theta)} \right] \\ &\quad - \mathbf{y}_l^T \mathbf{W}'_{l,k}{}^{(\theta)} \boldsymbol{\mu}_x^{(\theta+1)}, \end{aligned} \quad (63)$$

$$[\mathbf{C}_{\phi_l}''^{(\theta+1)}]_{k,k'} \equiv \text{tr} \mathbf{C}_x^{(\theta+1)} [\mathbf{W}'_{l,k}{}^{(\theta)}]^T \mathbf{W}'_{l,k'}{}^{(\theta)}. \quad (64)$$

Now, we obtain the well-approximated PM of \mathbf{x} as $\boldsymbol{\mu}_x^{(\infty)}$. Realistically, instead of $\boldsymbol{\mu}_x^{(\infty)}$, we use $\boldsymbol{\mu}_x^{(\theta+1)}$ when the following convergence condition holds,

$$\frac{\|\boldsymbol{\mu}_x^{(\theta+1)} - \boldsymbol{\mu}_x^{(\theta)}\|^2}{\|\boldsymbol{\mu}_x^{(\theta)}\|^2} < 10^{-5}, \quad \frac{\|\boldsymbol{\mu}_\phi^{(\theta+1)} - \boldsymbol{\mu}_\phi^{(\theta)}\|^2}{\|\boldsymbol{\mu}_\phi^{(\theta)}\|^2} < 10^{-5}. \quad (65)$$

V. EXPERIMENTAL RESULTS

The proposed method was evaluated using the following images and settings. We used five gray-scale images with a size of 40×40 pixels as shown in Fig. 2. From each image, $L = 10$ images with a size of 10×10 pixels were created following the parameters of the resolution enhancement factor $\alpha = 4$, Φ , and β . The transformation parameter Φ was randomly created according to the prior distribution in Eq.

TABLE I
ISNRs OF ESTIMATION RESULTS

Image	SNR (dB)	PSNR (proposed)	ISNR (bilinear)	ISNR (Kanemura)	ISNR (Babacan)
Lena	20	29.32 ± 0.38	7.20 ± 0.37	1.21 ± 0.50	0.23 ± 0.13
	25	30.50 ± 0.43	8.28 ± 0.43	1.40 ± 0.31	0.25 ± 0.24
	30	31.70 ± 0.54	9.44 ± 0.54	2.03 ± 0.70	0.53 ± 0.72
Cameraman	20	21.74 ± 0.24	4.61 ± 0.24	1.39 ± 0.36	0.15 ± 0.13
	25	22.52 ± 0.22	5.32 ± 0.22	1.73 ± 0.46	0.09 ± 0.13
	30	23.37 ± 0.30	6.15 ± 0.30	1.91 ± 0.31	0.00 ± 0.20
Pepper	20	29.66 ± 0.19	4.21 ± 0.18	0.22 ± 0.32	0.30 ± 0.16
	25	30.34 ± 0.46	4.76 ± 0.45	0.03 ± 0.35	0.76 ± 1.18
	30	31.10 ± 0.41	5.48 ± 0.41	0.07 ± 0.44	1.23 ± 1.18
Clock	20	23.14 ± 0.30	5.59 ± 0.30	1.63 ± 0.46	0.17 ± 0.14
	25	24.10 ± 0.35	6.48 ± 0.35	2.18 ± 0.59	0.16 ± 0.05
	30	25.20 ± 0.42	7.56 ± 0.42	2.83 ± 0.46	0.32 ± 0.18
Text	20	24.14 ± 0.46	5.94 ± 0.46	1.61 ± 0.43	0.08 ± 0.07
	25	25.81 ± 0.40	7.56 ± 0.41	2.55 ± 0.36	0.07 ± 0.06
	30	26.52 ± 0.52	8.25 ± 0.52	2.94 ± 0.32	0.03 ± 0.28

TABLE II
RMSES OF REGISTRATION ESTIMATION RESULTS

Image	SNR (dB)	RMSE (proposed)	RMSE (Kanemura)	RMSE (Babacan)
σ_x	20	0.088	0.124	0.116
	25	0.065	0.092	0.094
	30	0.061	0.075	0.095
σ_y	20	0.074	0.111	0.089
	25	0.063	0.081	0.103
	30	0.047	0.068	0.083
θ	20	0.006	0.006	0.006
	25	0.004	0.005	0.005
	30	0.003	0.003	0.004
γ	20	0.028	0.029	0.030
	25	0.029	0.029	0.031
	30	0.028	0.028	0.030

(18). The noise level parameter β was set for the signal-to-noise ratio (SNR) of 20, 25, and 30dB for each experiment. Samples of the created images are shown in Fig. 3.

Figure 4 shows the estimated images under SNR= 30dB. The resolution of each image appeared to be better than the corresponding observed image in Fig. 3.

Table I shows the quantitative results compared to those from the methods of bilinear interpolation, Kanemura et al. [10] and Babacan et al. [2]. Note that we added a slight modification to these methods because they employ slightly different models. For example, the original method [2] assumes the blurring parameter γ is known, so we set γ as the mean value of the true distribution for this method. Also, we introduced a strong prior for λ in the Kanemura method [10] in contrast to the original method because this parameter sometimes becomes negative. We evaluated the results with regard to the expectation and the standard deviation of the improvement in signal-to-noise ratio (ISNR) over 10 experiments on each image and for each SNR. ISNR is relative PSNR defined as

$$\text{ISNR} \equiv \text{PSNR}(\hat{x}; x) - \text{PSNR}(\tilde{x}; x), \quad (66)$$

where x is the true HR image, \tilde{x} is the image estimated by the baseline method, and \hat{x} is the image estimated by the method being evaluated. We see that the ISNRs of all the images estimated by the proposed method were better than those for other methods.

Also, we show the quantitative results compared to those about registration in table II. To evaluate the estimated registra-

tion parameters we use the root mean square error (RMSE). We see that the RMSEs of the proposed method were better than those of other methods at all noise levels.

VI. DISCUSSION

With regard to the observation model, we used the linear transformation and AWGN. Use of the linear transformation model in the proposed method is advantageous since an arbitrary transformation matrix $\mathbf{W}(\phi_l)$ can be employed because of the Taylor approximation. As for the transformation matrix, it can be constructed by multiplying three matrices: the warping, blurring, and downsampling matrices [2]. A disadvantage of this is that sub-pixel errors might accumulate. We prefer matrix construction via a continuous function [7]. In addition, we have improved this approach by introducing the elliptic theta function for the normalizing constant in Eq. (3). This normalizing constant provides fair pixel weights for both marginal and central areas of the HR image.

With regard to the HR image prior, the causal type of prior was first introduced by Kanemura et al. [11]; however, they seemed to be confused with respect to Eq. (7) and Eq. (13). The microstate energy function, or equivalently, the Hamiltonian, -based compound MRF prior offers the advantage of easy construction, but it usually has an exponential calculation cost $\mathcal{O}(2^{N_\eta})$ for the normalizing constant, or equivalently, the partition function, and this is an obstacle to direct calculation of the PM solution. Thus, the MAP solution has been used

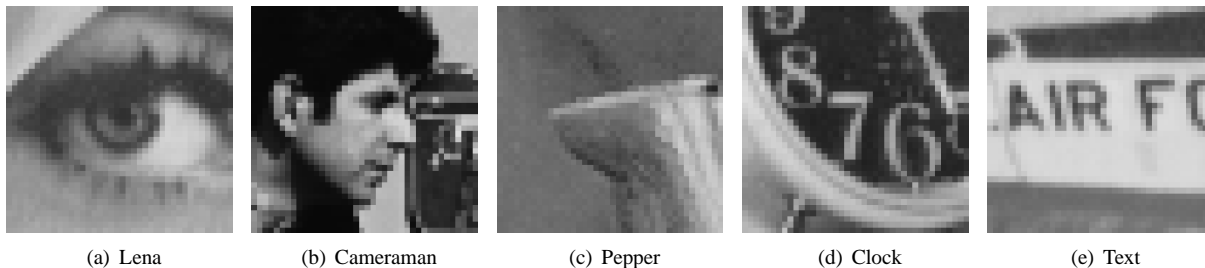


Fig. 2. Five original images used in the experiments

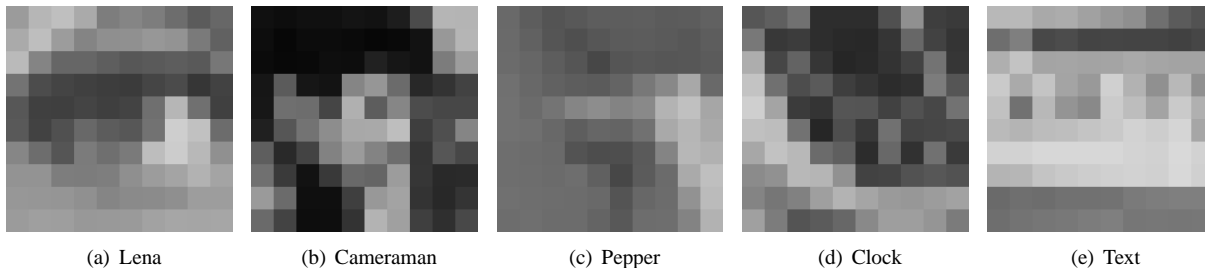


Fig. 3. Observed images when warped, blurred, downsampled by an enhancement factor of 4, and noised with SNR= 30dB AWGN

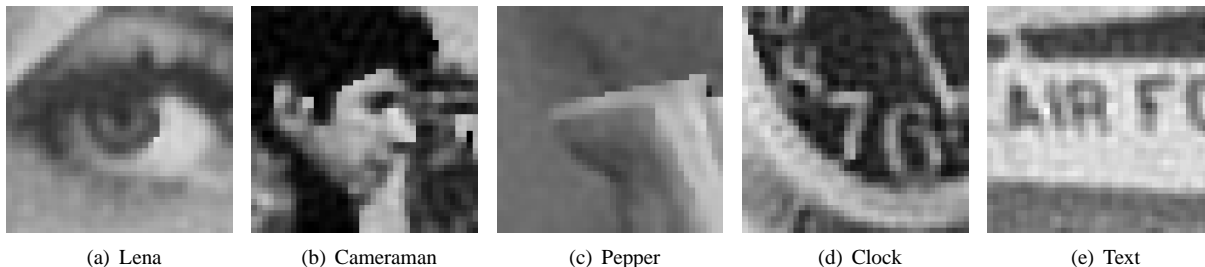


Fig. 4. Images estimated from the Fig. 3 observed images

in work elsewhere because the MAP solution is not affected by the normalizing constant. In contrast, the introduced causal type of prior of Eq. (7) has only a polynomial calculation cost $\mathcal{O}(N_x^3)$, which enables us to successfully apply the variational Bayes method to this problem.

With regard to the hyperparameter priors, we also improved the existing method. As the edge penalty parameter λ , Kanemura et al. [10] implicitly assumed $\lambda \in \mathcal{R}$, which leads to negative λ and consequently results in an edge-strewn image. We assumed $\lambda > 0$ by setting its prior according to a gamma distribution, resulting in an appropriate inference. As the smoothness parameter ρ , they practically fixed the value of ρ with a strongly informative prior. We chose a non-informative prior for ρ . As can be seen from the experimental results (Fig. 5), the inferred value of the PM of ρ showed wide variation, with an approximately 10-fold maximum-to-minimum ratio, depending on the original image. This result can be interpreted as meaning it is worth inferring ρ in each HR image. Furthermore, λ and κ respectively showed approximately 2-fold and 5-fold ranges of variation. Regarding the contrast parameter κ , they assumed $\kappa \equiv 0$, which leads to $|\mathbf{A}| = 0$ and results in an improper normalizing constant. While we assume $\kappa > 0$, which leads to a proper normalizing constant, we can consequently take the term of $\ln |\mathbf{A}|$ into account in the update equations in variational Bayes.

With regard to the prior distribution for the blurring parameter γ , we used a Gaussian distribution even though γ is a positive real number. This is because we selected a simpler expression. We have tried using the prior of the gamma distribution as γ , but the improvement was small. One disadvantage of this model is that the non-informative setting for this prior may lead to a nonsense result where the inferred γ is negative. Also, we employed a somewhat informative prior for γ . This is because the blurring parameter γ and the smoothness hyperparameter ρ are somewhat complementary. This means that the simultaneous estimation of γ and ρ is difficult. Tipping et al. [7] and Kanemura et al. [10] fixed ρ , and Babacan et al. [6] fixed γ .

With regard to the estimator, we logically derived the optimal estimator PM from the objective function of L2-norm-based PNSR. The widely used joint MAP estimator can be considered the optimal estimator for the all-or-none type objective function,

$$\operatorname{argmax}_{\hat{\mathbf{z}}} \langle \delta(\hat{\mathbf{z}} - \mathbf{z}) \rangle_{p(\mathbf{z}|\mathbf{Y})} = \operatorname{argmax}_{\mathbf{z}} p(\mathbf{z}|\mathbf{Y}), \quad (67)$$

where δ is the Dirac delta or Kronecker delta function. Generally, this type of objective function is nonsensical for continuous variables because it is measure zero. If all the random variables in the posterior distribution are discrete, or if

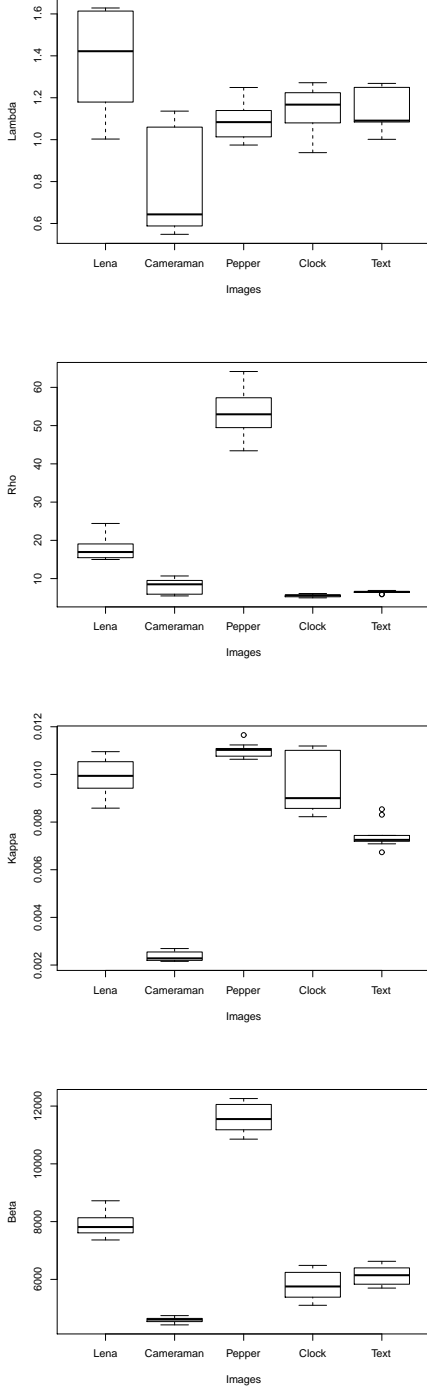


Fig. 5. Distributions of the PM of the hyperparameters of λ , ρ , κ , and β under SNR= 30dB noise

we can assume some smoothness of the posterior distribution, a joint MAP solution will have meaning. Instead of the L2-norm-based objective function of PSNR, the L1-norm (mean absolute error) -based PSNR is sometimes employed. In such cases, the median of the posterior distribution is generally the optimal estimator. The marginal ML, or equivalently, type II maximum likelihood or empirical Bayes, infers the registration

parameters and other hyperparameters:

$$[\tilde{\lambda}, \tilde{\rho}, \tilde{\kappa}, \tilde{\beta}, \tilde{\Phi}] \equiv \underset{\lambda, \rho, \kappa, \beta, \Phi}{\operatorname{argmax}} p(\mathbf{Y}|\lambda, \rho, \kappa, \beta, \Phi). \quad (68)$$

If these parameters have priors, such a method is called marginal MAP. The HR image and sometimes the edge information are then inferred as MAP,

$$\tilde{\mathbf{x}} \equiv \underset{\mathbf{x}}{\operatorname{argmax}} \max_{\boldsymbol{\eta}} p(\mathbf{x}, \boldsymbol{\eta}|\mathbf{Y}, \tilde{\lambda}, \tilde{\rho}, \tilde{\kappa}, \tilde{\beta}, \tilde{\Phi}), \quad (69)$$

or PM. For such a two-step inference, it is difficult to calculate back the objective function.

With regard to the Taylor approximation for the transformation matrix $\mathbf{W}(\phi_l)$, we used the first-order approximation in Eq. (31) because it is more stable than the second-order approximation. This first-order approximation was proposed by Villena et al. [6]. The second-order approximation was proposed by Pickup et al. [3] and they obtained good results. We have also tried the second-order approximation, but it sometimes made the algorithm unstable. This is because a second-order approximation sometimes fails to produce a positive definite matrix for the covariance matrix $\Sigma_{\mathbf{x}}$.

With regard to the Taylor approximation for $\ln |\mathbf{A}(\boldsymbol{\eta}, \rho, \kappa)|$ and $\ln \operatorname{logistic}(\lambda)$, we introduced the first-order approximation around $[\boldsymbol{\eta}, \ln \rho, \ln \kappa] = [\boldsymbol{\mu}_{\boldsymbol{\eta}}^{(\theta)}, \ln \mu_{\rho}^{(\theta)}, \ln \mu_{\kappa}^{(\theta)}]$ and $\ln \lambda = \ln \mu_{\lambda}^{(\theta)}$, respectively, in Eqs. (34) and (37). Note that Taylor expansion not with respect to ρ, κ, λ , but with respect to $\ln \rho, \ln \kappa, \ln \lambda$ is our key idea to solve the conjugate prior problem. Indeed, we could successfully derive the terms originating from $\ln |\mathbf{A}|$ in update equations (46), (54), and (56). Kanemura et al. [11] ignored the term of $\ln |\mathbf{A}|$ because of the high calculation cost, and this would result in less accurate inference. As for $\boldsymbol{\eta}$, we implicitly assumed that $\boldsymbol{\eta}$ is not a binary vector but a continuous vector, and did the differentiation. This assumption is based on Eq. (11). If we employ another assumption – i.e., replacement of $\eta_{i,j}$ with $\eta_{i,j}^2$ in Eq. (11) – Eq. (11) has the same meaning, but the result of Taylor approximation will differ from the current form.

VII. CONCLUSION

In this paper, we proposed a Bayesian image super-resolution (SR) method with a causal Gaussian Markov random field (MRF) prior. We improved existing models with respect to three points: 1) the combined transformation model through a preferable normalization term using the elliptic theta function, 2) the causal Gaussian MRF model through introducing a contrast parameter κ , which provides an effective normalizing constant including $\ln |\mathbf{A}|$, and 3) the hyperparameter prior model through application of a gamma distribution for the edge penalty parameter λ , which prevents an unfavorable edge-strewn image. We then logically derived the optimal estimator, not the joint maximum a posteriori (MAP) or marginalized maximum likelihood (ML) but the posterior mean (PM), from the objective function of the L2-norm (mean square error) -based peak signal-to-noise ratio (PSNR). The estimator is numerically determined by using variational Bayes. We solved the conjugate prior problem in variational Bayes by introducing three Taylor approximations.

Other than these Taylor approximations, we did not use any approximations such as ignoring the term $\ln |A|$. Experimental results showed that the proposed method is superior to existing methods in accuracy.

ACKNOWLEDGMENTS

This work was partially supported by a Grant-in-Aid for Scientific Research on Priority Areas (No. 18079012) and by a Grant-in-Aid for Young Scientists (B) (No. 21700263) of the Japanese Ministry of Education, Culture, Sports, Science and Technology.

REFERENCES

- [1] Tsai, R.Y. and Huang, T.S., "Multiframe image restoration and registration," in *Advances in computer vision and image processing*, CT:JAI Press, vol. 1, pp. 317–339, Greenwich, 1984.
- [2] S. D. Babacan, R. Molina, A. K. Katsaggelos, "Variational Bayesian Super Resolution," *IEEE Transactions on Image Processing*, vol. 20, no. 4, pp. 984–999, 2011.
- [3] L. C. Pickup, D. P. Capel, S. J. Roberts, and A. Zisserman, "Bayesian Image Super-Resolution, continued," in *Advances in NIPS 19*, MIT Press, 2007.
- [4] Hardie, R.C., Barnard, K.J., and Armstrong, E.E., "Joint Map registration and high resolution image estimation using a sequence of undersampled images," *IEEE Trans. Image Process.*, vol. 6, no. 12, pp. 1621–1633, 1997.
- [5] R. Molina, M. Vega, J. Abad, and A. K. Katsaggelos, "Parameter Estimation in Bayesian High-Resolution Image Reconstruction With Multisensors," *IEEE Transactions on Image Processing*, vol. 12, no. 12, pp. 1655–1667, 2003.
- [6] S. Villena, M. Vega, S.D. Babacan, R. Molina, and A. K. Katsaggelos, "Image Prior Combination in Super-resolution Image Registration & Reconstruction," *IEEE International Workshop on Machine Learning for Signal Processing (MLSP)*, pp. 355–360, 2010.
- [7] M. E. Tipping, and C. M. Bishop, "Bayesian image super-resolution," in *Advances in NIPS 15*, pp. 1279–1286, MIT Press, 2003.
- [8] S. Geman, and D. Geman, "Stochastic relaxation, Gibbs distributions, and the Bayesian restoration of images," *IEEE Trans. on Pattern Analysis and Machine Intelligence*, vol. PAMI-6, no. 6, pp. 721–741, 1984.
- [9] R. Molina, J. Mateos, A. K. Katsaggelos, and M. Vega, "Bayesian multichannel image restoration using compound Gauss-Markov random fields," *IEEE Transactions on Image Processing*, vol. 12, no. 12, pp. 1642–1654, 2003.
- [10] A. Kanemura, S. Maeda, and S. Ishii, "Hyperparameter Estimation in Bayesian Image Superresolution with a Compound Markov Random Field Prior," *IEEE International Workshop on Machine Learning for Signal Processing (MLSP)*, pp. 181–186, 2007.
- [11] A. Kanemura, S. Maeda, and S. Ishii, "Superresolution with compound Markov random fields via the variational EM algorithm," *Neural Networks*, vol. 22, pp. 1025–1034, 2009.
- [12] R. Chellappa, and A. Jain, *Markov random fields: Theory and application*, San Diego, CA: Academic Press, 1991.
- [13] F.-C. Jeng, and J. W. Woods, "Compound Gauss-Markov random fields for image estimation", *IEEE Transactions on Signal Processing*, vol. 39, no. 3, pp. 683–697, 1991.
- [14] H. Attias, "Inferring parameters and structure of latent variable models by variational Bayes," in *Proc. UAI*, San Francisco, CA, pp. 21–30, Morgan Kaufmann, 1999.
- [15] F.-C. Jeng, and J. W. Woods, "Simulated annealing in compound Gaussian random fields," *IEEE Transactions on Information Theory*, vol. 36, no. 1, pp. 94–107, 1990.